

FPGA Implementation of Image Compression using DPCM and FBAR

Yan Wang, Shoushun Chen and Amine Bermak
Smart Sensory Integrated Systems Lab
Electronic and Computer Engineering Department
Hong Kong University of Science and Technology
Clear Water Bay, Kowloon, Hong Kong, SAR.
Email: wongyin,dazui,eebermak@ust.hk

Abstract—This paper presents a hybrid image compression algorithm based on a novel adaptive quantization algorithm referred to as Fast Boundary Adaptation Rule (FBAR) combined with the Differential Pulse Code Modulation (DPCM) technique. The proposed image compression technique results in enhanced image quality as compared to FBAR-based compression. Our proposed system is still much simpler compared to other transform coding for image compression, such as JPEG that are widely adopted as the international standard. This made our system a viable candidate for developing on chip image sensor with data compression processor. The proposed compression algorithm was validated through FPGA implementation and was interfaced with a CMOS image sensor for real life applications. An 8:1 compression ratio with fairly good image quality were achieved with an average of 30dB PSNR as compared to 25dB for FBAR.

I. INTRODUCTION

Image compression is a very important processing in many digital imaging applications such as mobile phones, PDAs, or even medical image acquisition apparatus, such as the camera-pill [1]. Video and image applications require intensive data acquisition, storage, and processing in order to transmit high quality images through limited bandwidth. Data compression has relieved the burden of image transmission and storage at the cost of extra computationally extensive processing [2]. There are numerous algorithms for data compression, usually with complicated transform coding, which requires large power consumption and large silicon area. Data compression is still the most expensive process for hardware implementation in digital camera applications [3].

In this paper, an FPGA implementation of a compression processor based on the boundary adaptation scheme combined with the differential pulse code modulation (DPCM) are proposed. In the proposed system, data is first acquired from a custom image sensor followed by a prediction stage, a quantization stage and finally a reconstruction stage is used on the encoder side before transmitting the compressed data to the decoder. As the adaptive quantization process is the same for both encoder and decoder, there is no need to send extra bits of information for the decoding and the reconstruction process. In order to illustrate the applicability and efficiency of this algorithm, FPGA implementation is demonstrated and interfaced with a CMOS image sensor.

The remainder of this paper is organized as follows. Section II introduces the FBAR algorithm for adaptive quantization. Section III presents the predictive compression algorithm - differential pulse code modulation. Section IV describes the MATLAB simulation results and the FPGA hardware implementation of our proposed compression system. Section V concludes this work.

II. FAST BOUNDARY ADAPTATION RULE

An ordinary N -point scalar quantizer is a mapping from a scalar-valued signal x into one of N reconstruction levels y_1, y_2, \dots, y_N . The quantizer is specified by $N - 1$ decision levels, N quantization intervals, and N reconstruction levels. The N quantization intervals are N regions denoted as R_1, R_2, \dots, R_N . If $x \in R_j$, then $Q(x) = y_j$. Quantization process thus inevitably introduces quantization error when the number of quantization intervals is less than the number of bits needed to represent any element in a whole set of data. The most commonly used distortion measure is the r^{th} power law distortion:

$$d(x, Q(x)) D_r \equiv \sum_{i=1}^N |x - y_i|^r p(x) dx \quad (1)$$

If a distortion measure $d(x, Q(x))$ is minimized, the quantizer is said to be optimal.

The Fast Boundary Adaptation Rule (FBAR) was developed to minimize the r^{th} power law distortion. The FBAR [4] algorithm adjusts all the boundaries or the so called decision levels of the quantizer each time when a pixel value falls into a specific quantization interval. Therefore, there is no need to know the image statistics before setting the decision levels and quantization levels for the quantizer.

Figure 1 illustrates the operation principles of the fast boundary adaptation rule for 3-bit quantizer. As it is a 3-bit quantizer, there are totally $N = 2^3 = 8$ quantization intervals. R_1 and $R_{8=N}$ are called overload (open) quantization interval, while $R_i, i = 2, 3, \dots, 7$ are called granular (closed) quantization intervals. When a pixel value falls into a quantization interval, all the boundaries will be shifted to get closer to that interval. The amount of shift is defined by the following

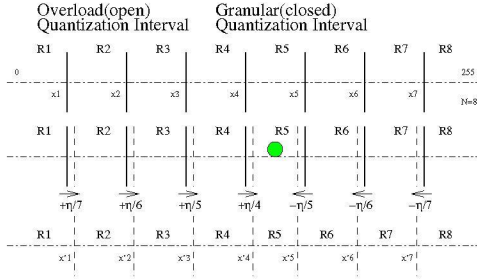


Fig. 1. Operation principle of The Fast Boundary Adaptation Rule for quantizer with 8 quantization levels.

equation:

$$\Delta x_j = \eta \left(\sum_{k=j+1}^N \delta_k^r \frac{\Pi_{R_k}}{N-j} - \sum_{k=1}^j \delta_k^r \frac{\Pi_{R_k}}{j} \right) \quad (2)$$

$j = 1, 2, \dots, N-1$, $\delta_i = x_i - x_{i-1}$, $r = 0$, and Eta η is the learning rate.

$\Pi_{R_i} = \begin{cases} 1 & \text{if } x \in R_i \\ 0 & \text{if } x \notin R_i. \end{cases}$ indicates the membership function.

III. DIFFERENTIAL PULSE CODE MODULATION

The direct quantization towards every pixel usually does not perform very well and does not produce very satisfactory image quality because of the unpredictable histogram of pictures. However, in traditional predictive image compression techniques, the quantization is usually performed towards the residual image. The residual image is obtained through subtracting the current pixel value with its prediction. The inter-pixel redundancy of closely spaced pixels can be eliminated through this technique, which is called Differential Pulse Code Modulation [5]. Its efficiency and computational simplicity have made it a strong competitor compared with the extensively adopted transform coding.

A. DPCM Operation Mechanism

Denote the pixel value along a row of an image as $f_i, i = 1, 2, \dots, m$, where m is the total number of pixels within the row. If the immediately preceding pixel value f_{i-1} is used as the prediction of the current pixel, then $\hat{f}_i = f_{i-1}$, in which \hat{f}_i denotes the prediction value. Then the residual signal $d_i = f_i - \hat{f}_i = f_i - f_{i-1}$ can be obtained.

From Figure 2, It is easy to get an intuitive scrutiny of why it is much better to code the residual image than to the original image. The histogram of residual image is symmetric with respect to zero and has significantly smaller dynamic range than that of the original image. It is noticeable that although the dynamic range of the residual image is theoretically doubled, from 256 ([0, 255]) to 512 ([-255, 255]), the variance of the residual signal is actually much smaller: the entropy is 7.4 for the original signal and 5.0 for the residual signal.

In a typical DPCM system, there are mainly two subsystems: Encoder in the transmitter side and Decoder in the receiver side. However, the decoding algorithm should always

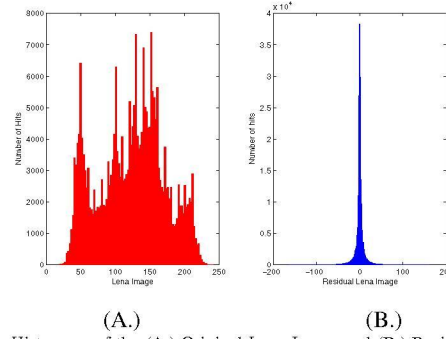


Fig. 2. Histogram of the (A.) Original Lena Image and (B.) Residual Image

be included in the encoder side in order to eliminate the cumulative quantization error, as will be explained in the next section.

For the case of simple encoder without any decoding mechanism included, the error analysis is as follows. Denote \hat{d}_i as the quantized version of the residual signal d_i , therefore, $\hat{d}_i = Q(d_i) = d_i + err_q$, where err_q represents the quantization error. Let \bar{f}_i be the reconstructed pixel value and \hat{f}_i be the predicted signal. In such system, the immediately preceding pixel value is used as the prediction value. For $i = 1$, $d_1 = f_1 - f_0$, and $\hat{d}_1 = d_1 + err_{q,1} \Rightarrow \bar{f}_1 = f_0 + \hat{d}_1 = f_1 + err_{q,1}$. Similarly, for $i = 2$, $\bar{f}_2 = f_2 + err_{q,1} + err_{q,2}$. Therefore, in general, $\bar{f}_i = f_i + \sum_{j=1}^i err_{q,j}$.

This phenomenon of cumulative quantization error happens because of the existence of unbalanced information between the receiver and the transmitter. As only the reconstructed signal can be available at both sides, the decoding process are designed to be employed in the encoder to address the problem of cumulative quantization noise. In this scheme, the previous reconstructed pixel value \bar{f}_{i-1} is used as the predictor \hat{f}_i , thus, $\hat{f}_i = \bar{f}_{i-1}$, $\bar{f}_i = \bar{f}_{i-1} + d_i$ and $d_i = f_i - \bar{f}_{i-1}$. For $i = 1$, $d_1 = f_1 - f_0$, and $\hat{d}_1 = d_1 + err_{q,1} \Rightarrow \bar{f}_1 = f_0 + \hat{d}_1 = f_1 + err_{q,1}$ and for $i = 2$, we can deduce $\bar{f}_2 = f_2 + err_{q,2}$. In a more general way, we can write, $\bar{f}_i = f_i + err_{q,i}$. One can conclude that having both the encoder and decoder working in the same way, the accumulated quantization error can be eliminated.

B. DPCM Predictor

In practical DPCM system, the current pixel value is first predicted from the previous reconstructed values. The difference between the current pixel and its predicted value is then quantized, coded, and transmitted to the receiver, which is in the decoder side. The same decoding algorithm is implemented both in the encoder and in the decoder sides. However, more complicated algorithm for prediction is usually introduced in the general DPCM system. The prediction of current pixel f_i is denoted as \hat{f}_i , which is a linear combination of the n previous reconstructed signals: $\bar{f}_{i-1}, \bar{f}_{i-2}, \dots, \bar{f}_{i-n}$. We can define $\hat{f}_i = \sum_{j=1}^n a_j \bar{f}_{i-j}$ with $a_j, j = 1, 2, \dots, n$ being the set of real coefficients. The prediction error, e_p , is defined as $e_p = f_i - \hat{f}_i$. The mean square prediction error, MSE_p is

defined as

$$MSE_p = E[(\epsilon_p)^2] = E\left[\left(f_i - \sum_{j=1}^n a_j \bar{f}_{i-j}\right)^2\right] \quad (3)$$

The design of optimum prediction refers to the determination of a set of coefficients a_j , $j = 1, 2, \dots, n$ such that the mean square prediction error, MSE_p is minimized. By taking the differentiation of MSE_p with respect to coefficients a_j , the following condition (orthogonality condition) $E[e_p \cdot \bar{f}_{i-j}] = 0$ must be satisfied for $j = 1, 2, \dots, n$. The interpretation of this equation is that the prediction error e_p must be orthogonal to all the preceding samples: \bar{f}_{i-j} , $j = 1, 2, \dots, n$. The calculation is usually quite difficult in practice, therefore, some widely adopted linear predictors were used as reported in Table I. Note that $A = \bar{f}(x, y - 1)$, $B = \bar{f}(x - 1, y)$, and $C = \bar{f}(x - 1, y)$.

TABLE I
PREDICTORS USED IN OUR DPCM SYSTEM.

Predictor	Definition
P_1	$\hat{f}(x, y) = A$
P_2	$\hat{f}(x, y) = 0.75A + 0.75C - 0.5B$
P_3	$\hat{f}(x, y) = 0.9A + 0.9C - 0.81B$
P_4	$\hat{f}(x, y) = A + C - B$
P_5	$\hat{f}(x, y) = 0.5(A + C)$
P_6	$\hat{f}(x, y) = \begin{cases} \max(A, C) & B \geq \max(A, C); \\ \min(A, C) & B \leq \min(A, C); \\ A + B - C & \text{otherwise.} \end{cases}$
P_7	$\hat{f}(x, y) = \begin{cases} A & B - C < A - B ; \\ C & \text{otherwise.} \end{cases}$

P_1 to P_5 represent simple fixed coefficient predictors [7], while P_6 and P_7 represent adaptive predictors. The predictor P_6 is adopted directly from JPEG-LS standard [6], which is a lossless compression standard proposed by JPEG committee and P_7 is the Graham's predictor [7].

IV. COMBINED FBAR AND DPCM SYSTEM

In our proposed image compression scheme, FBAR $_{r=0}$ quantization algorithm was incorporated with the DPCM system to achieve fairly good image quality with the compression ratio of 8:1. With the same compression ratio, the proposed system enhanced the image quality as compared to FBAR only compression based system but at the cost of extra processing unit introduced by DPCM algorithm. The main structure and the overall design of the hybrid system is shown in Figure 3.

The input signal to our system is the data from an image sensor using a raster scan scheme. Each pixel value is then subtracted by its prediction to form the residual signal that is then to be quantized by FBAR quantizer. The code word at the output of FBAR is transmitted through the channel and at the same time decoded to get the quantized version of residual signal before feeding back the data for the next iteration (refer to Figure 3). Both the decoder and the encoder contain the same decoding mechanism. The predictor P_5 of Table I, was used in our FPGA implementation. In this predictor, the average of the upper and the left pixels immediately adjacent

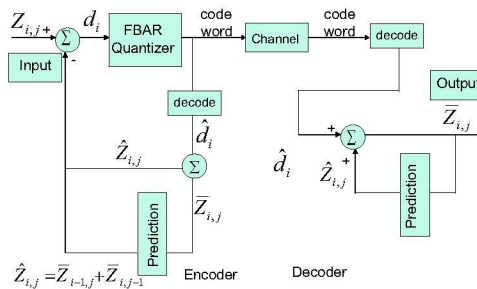


Fig. 3. Our proposed compression system combining FBAR and DPCM.

to the reconstructed pixel is used as the prediction value. The performance of all predictors are compared for different images and reported in Table II. We can note that despite its simplicity, predictor P_5 achieves very good performance.

TABLE II
COMPARISON BETWEEN OUR PROPOSED COMPRESSION SCHEME AS REPORTED IN FIG. 3 AND STAND-ALONE FBAR IN TERMS OF PSNR FOR THE SAME COMPRESSION RATIO.

Predictors Images	FBAR	P_1	P_2	P_3	P_4	P_5	P_6	P_7
engine	22.3	21.5	22.5	21.1	19.4	22.8	22.7	22.2
kodium22	26.9	27.2	30.1	29.7	27.7	29.1	30.7	29.9
leaves	25.0	26.5	28.6	27.7	25.9	28.3	28.8	28.3
satelv	26.8	26.9	28.4	27.1	25.7	29.2	28.5	27.6
Sydney	24.5	24.6	29.1	28.4	26.7	27.5	29.3	28.1
watch	27.3	28.9	30.6	29.4	27.2	30.6	31.0	30.2
yosemite	26.9	27.1	28.9	27.9	26.3	29.1	28.8	27.8
KODIE	23.8	27.6	30.2	29.6	27.7	29.5	30.2	29.6
zelda	30.2	33.9	38.5	38.0	35.8	36.9	38.6	37.2
parrots	27.0	29.2	32.5	31.4	28.9	32.1	32.6	31.2
picnic02	26.4	30.0	32.6	31.9	29.4	31.7	32.5	31.6
picnic03	25.5	28.3	32.1	31.2	29.0	30.9	31.9	30.8
rafting	26.4	26.8	28.9	27.9	26.0	28.7	28.8	28.0
monarch	24.0	24.8	28.7	28.1	26.3	27.7	28.1	26.8
mtsunset	30.6	30.9	33.1	31.8	30.1	33.2	32.9	32.1
kodakBus	25.2	26.0	29.0	28.3	26.4	28.1	29.0	28.0
iptcte02	18.9	19.3	21.9	21.9	20.6	20.6	22.4	22.0
frymire	18.8	17.9	19.0	18.3	17.2	19.1	19.1	18.9
fruits	25.3	26.5	30.2	29.5	27.0	28.9	30.1	29.1
bird	26.7	29.6	32.4	31.4	29.0	31.5	32.4	31.9
gold	28.9	30.0	33.5	32.5	30.8	32.5	33.7	32.6
lena	25.7	29.1	32.4	31.7	29.3	31.3	32.3	31.6
baboon	26.9	26.4	27.1	25.7	24.0	27.8	27.3	26.5
barb	26.8	26.9	29.5	27.9	26.1	29.6	29.8	28.9
Peppers	25.2	27.2	30.5	32.8	31.4	28.8	34.2	33.1
Tiffany	28.6	30.3	33.3	32.8	31.2	32.3	33.9	33.3
sailboat	24.9	27.7	31.4	30.6	29.0	30.5	31.3	29.8
AVERAGE	25.7	27.0	29.8	29.0	27.2	29.2	30.0	29.1

It is clear from Table II that an improvement in terms of image quality at about 5dB is achieved using our proposed system as compared to a stand-alone FBAR. Our proposed system was implemented on an FPGA platform (based on Xilinx Virtex II) and interfaced with an image sensor. The schematic of the DPCM with 1-bit FBAR system is illustrated in figure 4. The schematic shows boundary point adaptation block which is used to compare the pixel value with the boundary point and to perform adjustment according to the comparison results. For fast tracking of the input signal an adaptive step size is used as illustrated in η Adaptation unit.

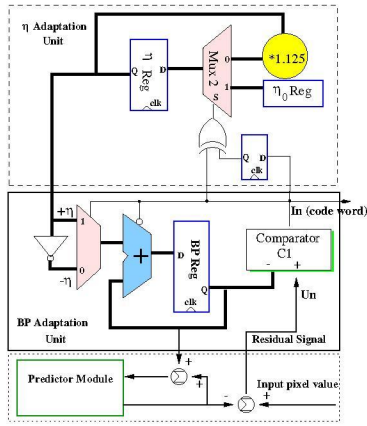


Fig. 4. The 1-bit FBAR and DPCM Encoder Circuit with adaptive η .

The platform was tested using sample 128×128 still images. The compressed data at the output of our system were captured and stored in the Smart Media Card of the FPGA board. The stored data were then sent to the PC in which the decoding process is performed. The predictor $P5$ was adopted because it performs quite well and is the simplest predictor that can be easily configured in hardware. The first pixel of each image was faithfully transmitted to the receiver and the prediction value for the pixels located in the first row uses only the adjacent left value while the predictor for the pixels located in the first column uses only the upper pixel. Figure 5 shows some sample images acquired from the FPGA platform. Top figure are the original figures while the bottom are the reconstructed images achieving about 8:1 compression ratio and a PSNR figure of about 30dB.

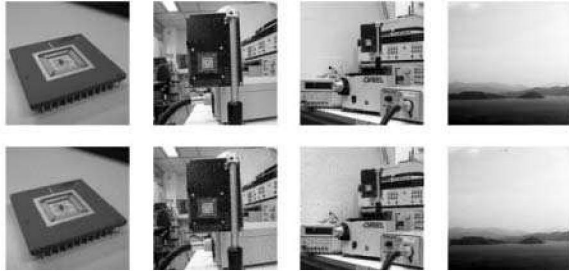


Fig. 5. Top images are the original images capture from our sensor. Bottom images are the reconstructed images where the compression is performed on our FPGA platform while the decoding is performed off-line using a PC.

Our system was successfully implemented in an FPGA and interfaced with an image sensor. Table II presents the FPGA design summary report for our system.

TABLE III
FPGA DESIGN SUMMARY REPORT

Logic Utilization	Used	Available	Utilization
Number of Slice Flip Flops	2169	28672	7%
Number of 4 input LUTs	9089	28672	31%
Frequency (MHz)	25		

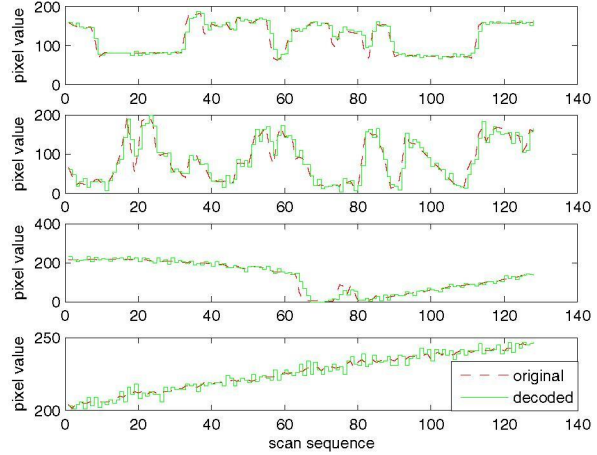


Fig. 6. Row original and reconstructed signals for the four images shown in Figure 5. Top to bottom figures correspond to row signals of left to right images represented in Figure 5.

V. CONCLUSION

This paper presents a hardware friendly image compression algorithm which consists of FBAR backward adaptation algorithm followed by DPCM compression technique. The MATLAB simulation results of this hybrid algorithm shows improved performance by an average of 5dB PSNR for the same compression ratio as compared to a stand-alone FBAR. Even though the added DPCM block requires extra hardware resources, it was shown that use of appropriate predictor can lead to hardware simplification. The proposed compression algorithm was implemented on an FPGA platform and interfaced to an image sensor. The simplicity of the algorithm makes it a very suitable candidate for on-chip compact and low power image compression algorithm that can be integrated with a CMOS image sensor.

ACKNOWLEDGMENT

This work was supported by a grant from the Research Grant Council of Hong Kong SAR, Project Ref. HKUST610405

REFERENCES

- [1] G. Iddan, G. Meron, A. Glukhousky and P.Swain "Wireless capsule endoscopy", *Nature*, pp.405 - 407, 2000.
- [2] A. Olyaei, R. Genov, "Mixed-Signal Harr Wavelet Compression Image Architecture", *Midwest Symposium on Circuits and Systems (MWSCAS'05)*, Cincinnati, Ohio, 2005
- [3] Kawahito *et AL*, "CMOS Image Sensor with Analog 2-D DCT-Based Compression Circuits", *IEEE Journal of Solid-State Circuits*, Vol. 32, No.12, pp.2029 - 2039, December 1997.
- [4] D. Martinez and M. M. Van Hulle, "Generalized Boundary Adaptation Rule for Minimizing r th Power Law Distortion in High Resolution Quantization", *Neural Networks*, Vol.8, No.6, pp.891 -900, 1995.
- [5] K. Sayood, "Introduction to Data Compression", 3rd Ed. *Morgan Kaufmann Publishers*, 2006.
- [6] M. Weinberger, *et AL*. "The LOCO-I Lossless Compression Algorithm", *Technical Report HPL-98-193*, HP lab, Nov. 1998.
- [7] Arun N. Netravali and Barry G. Haskell, "Digital pictures : representation, compression, and standards", *Plenum Press*, 1995.